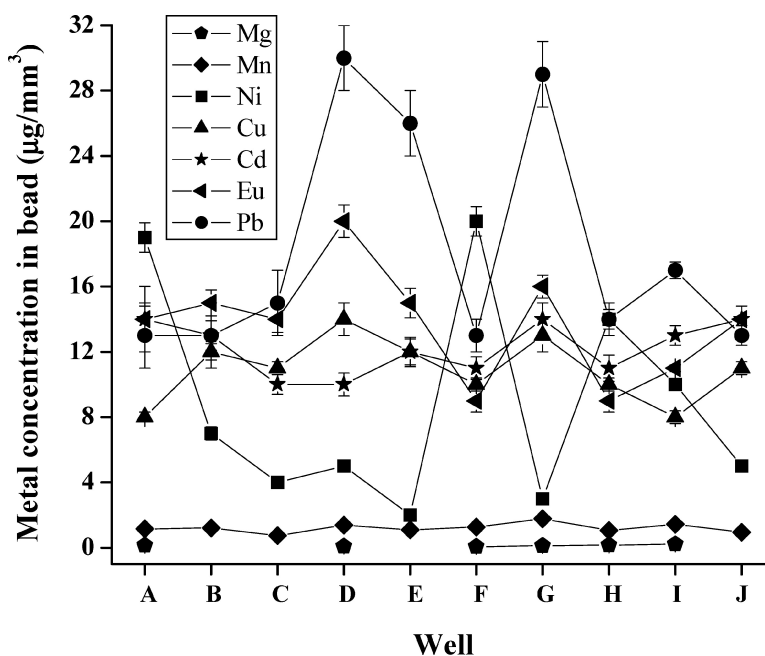


## Quantitative Determination of Single-Bead Metal Content from a Peptide Combinatorial Library

Jacqueline L. Stair, Brianna R. White, Adam Rowland, and James A. Holcombe

*J. Comb. Chem.*, 2006, 8 (6), 929-934 • DOI: 10.1021/cc060100m • Publication Date (Web): 06 October 2006

Downloaded from <http://pubs.acs.org> on March 22, 2009



### More About This Article

Additional resources and features associated with this article are available within the HTML version:

- Supporting Information
- Links to the 2 articles that cite this article, as of the time of this article download
- Access to high resolution figures
- Links to articles and content related to this article
- Copyright permission to reproduce figures and/or text from this article

[View the Full Text HTML](#)



**ACS Publications**  
 High quality. High impact.

# Quantitative Determination of Single-Bead Metal Content from a Peptide Combinatorial Library

Jacqueline L. Stair, Brianna R. White, Adam Rowland, and James A. Holcombe\*

*Department of Chemistry and Biochemistry, University of Texas at Austin, Austin, Texas 78712*

*Received July 18, 2006*

An electrothermal vaporizer inductively coupled plasma mass spectrometer (ETV-ICPMS) was used to quantitatively screen metals bound to single polystyrene (TentaGel) beads with immobilized oligopeptides. Tests were performed using ETV-ICPMS to screen a series of identical beads as well as a series of combinatorial library beads exposed to a multimetal solution composed of  $\text{Mg}^{2+}$ ,  $\text{Mn}^{2+}$ ,  $\text{Ni}^{2+}$ ,  $\text{Cu}^{2+}$ ,  $\text{Cd}^{2+}$ ,  $\text{Eu}^{2+}$ , and  $\text{Pb}^{2+}$ . The residual metal content remaining bound to the beads after acid extractions was also analyzed by solid sampling of the entire bead using oxygen ashing in the ETV. Nine beads (80 mesh, 0.25 mmol  $\text{g}^{-1}$  nominal capacity) containing covalently attached polyaspartic acid (PLAsp;  $n = 20$ ) showed metal extract concentrations in the range of 4–130 ng  $\text{mL}^{-1}$ . After normalizing by bead volume, the precision of capacity measurements in a single bead (7–14%) was primarily dictated by analysis error and contributions from bead diameter measurement with negligible contributions, surprisingly, from variations in site density from bead to bead. A sample combinatorial library of the sequence GXXGXXGXXGXX ( $X =$  cysteine, aspartic acid, or glutamic acid and  $G =$  glycine) (60 mesh, 0.25 mmol  $\text{g}^{-1}$  nominal capacity) was also used to demonstrate the utility of this method. Metal extract concentrations ranged from 1 to 1300 ng  $\text{mL}^{-1}$  with significant concentration variation between beads, indicating the individual selectivity on each bead. For these larger beads, analysis precision (i.e., capacity precision) was further improved to 3–10% due to the overall increase in bead metal content. Through metal extract determinations, ETV-ICPMS was shown to be a viable nondestructive tool for full metal characterization of “hit” sequences belonging to a combinatorial library.

## Introduction

The use of combinatorial libraries has allowed the evaluation of numerous variations to a chemical system in a shortened amount of time. Combinatorial approaches have been utilized in many fields, including catalysis,<sup>1,2</sup> chiral separations,<sup>3</sup> drug discovery,<sup>4,5</sup> and inorganic material synthesis.<sup>6,7</sup> In all approaches, one challenge is finding suitable ways to screen thousands of beads to obtain the desired information.

One recent area of growth is the use of peptide combinatorial libraries for identifying selective metal chelators.<sup>8</sup> In these libraries, one approach is to design or optimize the composition of a short, metal-binding peptide on the basis of information from a larger protein (such as a metallothionein<sup>9</sup>). One objective is to simplify the chelator without losing metal-binding capacity or specificity and, in some instances, perhaps even increasing selectivity. This is done using libraries in which specific amino acid positions along the peptide chain can be varied to increase and tune metal-binding capacity and specificity. There are many advantages to this approach,<sup>10,11</sup> including the design flexibility provided by 26 naturally occurring amino acid building blocks as well as the ease of peptide library synthesis. Beads with the desired metal-binding properties can then be sequenced using methods such as Edman degradation and mass spectrometry.

Screening beads from a combinatorial library for metal content has previously been achieved through colorimetric or fluorescent dyes complexing with the metal of interest<sup>12,13</sup> or by observing color changes due to metal–peptide complexation itself.<sup>14,15</sup> Although nondestructive, these approaches are largely qualitative and are usually limited to the analysis of one metal at a time. Nondestructive techniques are mandatory for later determination of peptide sequences. For metal remediation and reclamation, determining how well a chelator selects for or discriminates against particular species is often important and obtained through examining the binding of multiple metals simultaneously. Energy-dispersive X-ray spectroscopy on a scanning electron microscope has been previously used for multielemental analysis on single beads; however, beads must be initially flattened and then coated with a conductive material before analysis.<sup>16</sup> Recently, Havrilla and co-workers used micro X-ray fluorescence for both bulk and selective metal screening of beads exposed to metal solutions.<sup>17,18</sup> This approach involves minimal sample preparation, is nondestructive, and is capable of simultaneous multielemental screening of single beads. The relative metal composition is determined from point scans, elemental imaging on the surface of the bead, or both. Although this technique provides relative metal content at particular points within the bead, absolute metal content is more difficult to obtain.<sup>17</sup>

In the current study, electrothermal vaporization inductively coupled plasma mass spectrometry (ETV-ICPMS) is

\* To whom correspondence should be addressed. E-mail: holcombe@mail.utexas.edu.

used for the simultaneous quantitative determination of several metals extracted into solution from a single bead for purposes of characterizing binding properties of the peptide immobilized on the bead. The ETV exhibits excellent sensitivity (e.g., subpicogram or part per trillion detection limits) and is ideally suited for use with very small sample volumes ( $\leq 10 \mu\text{L}$ ). The mass analyzer used was a time-of-flight (TOF) system. The TOF mass analyzer allows for multielemental analysis with no loss in analytical duty cycle as the number of monitored masses increases.<sup>19</sup>

### Materials and Methods

**Chemicals.** All chemicals were reagent grade unless otherwise noted, and deionized distilled water was used to prepare solutions. All glassware and plasticware were soaked overnight in 4 mol L<sup>-1</sup> HNO<sub>3</sub> prior to use. The synthesis procedure for polyaspartic acid (PLAsp;  $n = 20$ ) was similar to that previously described,<sup>20</sup> and characterization using mass spectrometry showed the peptide was composed of 40% 20-residue form, 40% 19-residue form, and 20% 18-residue form. The combinatorial library (CPC Scientific) was composed of the sequence GXXGXXGXXGXX (X = cysteine, aspartic acid, or glutamic acid; G = glycine) and synthesized onto TentaGel Macrobeads (Rapp-Polymere MB 250 002) resin (60 mesh; 0.25 mmol g<sup>-1</sup>). Microwell plates (96 wells; 300  $\mu\text{L}$ ) were purchased from Fisher Scientific (21-377-203), adhesive sheets used to cover the wells were purchased from Nunc (236366), and Tacky Dot slides (glass slides with arrays of adhesive spots used to easily array microbeads) were purchased from SPI supplies (2388). Stock solutions of 1000  $\mu\text{g mL}^{-1}$  Cd<sup>2+</sup>, Ni<sup>2+</sup>, and Eu<sup>2+</sup> (Acros) and Pb<sup>2+</sup>, In<sup>2+</sup>, Cu<sup>2+</sup>, and Mn<sup>2+</sup> (SCP Science) standards in 2 and 4% HNO<sub>3</sub> were used to prepare both the multimetal-binding solution and the multimetal standards. For Mg<sup>2+</sup>, the metal solutions were prepared from a standardized solution of the reagent grade nitrate salt (J.T. Baker) in 1% (v/v) HNO<sub>3</sub> and 1% (v/v) HCl. A 0.2 mol L<sup>-1</sup> ammonium acetate (Aldrich) and 0.2 mol L<sup>-1</sup> (*N*-[hydroxyethyl]piperazine-*N'*-[2-ethanesulfonic acid]) (HEPES) (Acros) buffer were prepared and purified by passing the buffer through a 100–200 mesh Chelex 100 (BioRad) ion exchange column. These metals were selected to demonstrate the multimetal capability of this technique. Previous studies have shown that many of these metals should preferentially bind, whereas others have no affinity for the amino acids selected.<sup>21</sup> Ar was used for the ICP and sweep gas (Praxair, Austin, TX). Other reagents used included nitric acid (70%, redistilled 99.999%) (Sigma) and DL-1,4-dithiothreitol (99%) (DTT) (Acros).

**Metal Binding and Extraction.** Prior to metal binding, the combinatorial library beads were exposed to 0.02 mol L<sup>-1</sup> DTT in 0.02 mol L<sup>-1</sup> of HEPES buffer (pH 8.0) to reduce disulfide bonds that may have formed between cysteine groups. The DTT solution was deaerated with N<sub>2</sub> prior to use, and the reaction was allowed to proceed under constant mixing for 1 h. For both bead sets, ~50 beads were added to 20 mL of a deaerated multimetal solution composed of 20  $\mu\text{g mL}^{-1}$  Mg<sup>2+</sup>, Mn<sup>2+</sup>, Ni<sup>2+</sup>, Cu<sup>2+</sup>, Cd<sup>2+</sup>, Eu<sup>2+</sup>, and Pb<sup>2+</sup> in 0.02 mol L<sup>-1</sup> ammonium acetate buffer (pH 7.0). The reaction solution was allowed to react under constant

**Table 1.** ICP Operating Parameters

sample gas flow	1.15 L min <sup>-1</sup>
plasma gas flow	10.0 L min <sup>-1</sup>
auxiliary gas flow	0.90 L min <sup>-1</sup>
RF generator forward power	700 W
torch position (x)	8.0 mm
torch position (y)	0.3 mm
torch position (z)	-0.2 mm
skimmer potential	-1000 V
extraction lens	-1400 V
pushout plate	510 V
pushout grid	-540 V
reflectron	580 V
detector	3200 V
analyzer	<sup>24</sup> Mg, <sup>55</sup> Mn, <sup>58</sup> Ni, <sup>63</sup> Cu, <sup>114</sup> Cd, <sup>208</sup> Pb, <sup>153</sup> Eu
(primary isotopes used)	
confirmation isotope	<sup>25</sup> Mg, <sup>60</sup> Ni, <sup>65</sup> Cu, <sup>112</sup> Cd, <sup>206</sup> Pb, <sup>151</sup> Eu
(where applicable)	

mixing for 2 h. The beads were suction-filtered (no rinse) and dried under N<sub>2</sub>(g) overnight. The beads were then shaken onto a Tacky Dot slide for stereoscope measurements. Using microtweezers, individual beads were selected randomly from the Tacky Dot slide and placed into individual wells containing 100 ng  $\mu\text{L}^{-1}$  In in 250  $\mu\text{L}$  of 0.1 mol L<sup>-1</sup> of nitric acid. Indium was used as an internal standard in the ETV-ICPMS to correct for solvent evaporation as well as autosampler variation. The acid solution from wells exposed only to the microtweezers which were placed in the sticky substance of the Tacky Dot slide was used for blank measurements. Once all the beads were placed into the wells, the wells were covered with a sealing adhesive sheet. The beads were soaked in acid for 2 h with 15 min on/off sonication cycling. After 2 h, 100  $\mu\text{L}$  of the metal extract was transferred from the well into autosampler cups for elemental analysis. Multimetal standards were prepared with 100 ng  $\mu\text{L}^{-1}$  In in 250  $\mu\text{L}$  of 0.1 mol L<sup>-1</sup> of nitric acid. For oxygen ashing experiments, the standards were rerun under the new ETV parameters (described under ETV-ICPMS). After removing the nitric acid solution, water (150  $\mu\text{L}$ ) was added to each well containing a bead, and each bead was pipetted up with ~100  $\mu\text{L}$  of water and deposited into the ETV for elemental analysis.

**Stereoscope Measurements.** An Olympus (SZX12) stereoscope was used to obtain images of the beads arrayed on a Tacky Dot slide. Slide sections were labeled for easy identification of the bead regions. Immediately after a bead image was saved, an image of a stage micrometer (1 mm long and subdivided into 10  $\mu\text{m}$  increments) was taken at the same magnification. These images were used to determine the diameter of each bead prior to acid extraction for adjusting the metal capacities with respect to the bead volume.

**ETV-ICPMS.** Measurements were carried out on an Optimass 8000 inductively coupled plasma orthogonal acceleration time-of-flight mass spectrometer (GBC Scientific; Hampshire, IL). Operating parameters for the ICPMS are described in Table 1. Calibration was performed with the ETV prior to bead analysis using standard solutions containing the ions of interest. Calibrations were retaken before oxygen ashing experiments to account for changes in sensitivity due to the altered ETV parameters.

**Table 2.** ETV Heating Program

step	temperature (°C)	ramp time (s)	hold time (s)	dosing hole closed
dry	100	5	10	no
char	300	20	20	no
pause	50	3	15	yes
vaporize	2800	3	5	yes <sup>a</sup>
cool	50	14	0	yes <sup>a</sup>
clean	2800	1.3	3	no
cool	50	14	0	no

<sup>a</sup> Denotes mass spectrometry data collection.

The ICPMS was coupled to the ETV, a modified electrothermal atomizer and autosampler (Varian model GTA-95; Walnut Creek, CA) that has been previously described.<sup>22</sup> Each sample was measured in triplicate using 10- $\mu$ L injections. Pyrolytically coated graphite tubes were used as the vaporizer (Varian, part no. 6310001200). A valve system was utilized to separate the ETV from the ICP when material was not being vaporized (i.e., during drying and ashing cycles). During these steps, the instrument's sample gas flow was diverted directly into the torch. During analyte vaporization, the valves were toggled so that Ar gas flow was directed through the graphite tube to sweep analyte into the mass spectrometer. During this cycle, the dosing hole of the graphite furnace was plugged by means of a pneumatically activated graphite-tipped plunger. This also triggered data collection in the Optimass 8000. Analyte was carried to the ICP torch by 1 m of 6-mm-i.d. Tygon tubing. The ETV heating program is described in Table 2.

For oxygen ashing studies, the drying step was increased to 60 s to accommodate the increased sample volume of 100  $\mu$ L. During the oxygen ash step, air was used in place of Ar, passing through the furnace at a rate of  $\sim$ 1.2 mL/min, and the ash temperature was set to 800 °C (viz., dull red furnace appearance looking through dosing hole) for 20 s. After ashing, the furnace was cooled to room temperature with air still flowing through the furnace. After a 10-s Ar flush, the ETV was heated to a vaporization temperature of 2800 °C, and the signal was collected.

## Results and Discussion

**Metal Determination from Beads with Immobilized PLAsp.** To determine the precision of the ETV-ICPMS method, beads containing the same peptide sequence were analyzed. The bead set used for this study was immobilized PLAsp ( $n = 20$ ) that was reacted with a multimetal solution for 2 h as described earlier. Depending on the peptide sequence and resin material used for the analysis, careful determination of reaction times must be considered for equilibrium conditions to be met. On the basis of the diffusion of large dye molecules through TentaGel,<sup>23,24</sup> metal diffusion through TentaGel beads should occur in 15 min, and earlier studies suggested rapid metal-peptide binding kinetics.<sup>20</sup> After metal exposure and drying, a light image of the beads was taken using a stereoscope. All beads were medium blue in color after metal binding, indicating that each bead possessed the PLAsp and some complexed metal(s). A set of nine beads was taken from the slide after

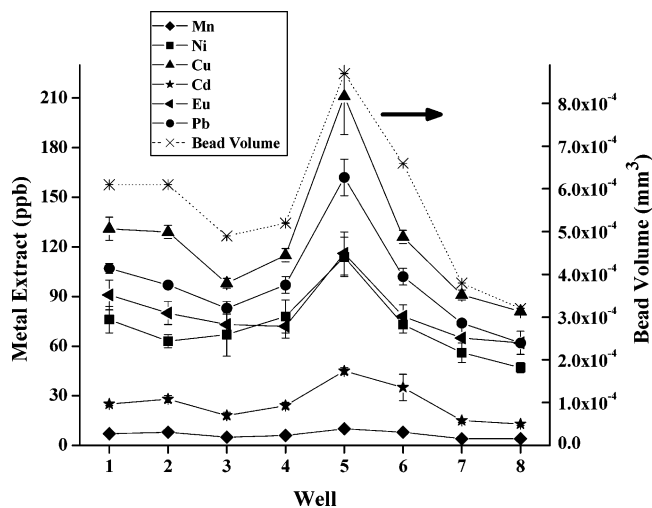


**Figure 1.** Concentration of metal extracted from single TentaGel-PLAsp beads and calculated bead volumes (right axis). The error bars represent  $\pm 1\sigma$  ( $n = 3$ ) based on error propagated using the analysis error of the sample, blank, and calibration solutions. (Two beads were present in well no. 5.)

**Table 3.** Bead-to-Bead Variation in Metal Extract Before and After Adjusting for Bead Volume<sup>a</sup>

element	Mn <sup>2+</sup>	Ni <sup>2+</sup>	Cu <sup>2+</sup>	Cd <sup>2+</sup>	Pb <sup>2+</sup>	Eu <sup>2+</sup>
	%	%	%	%	%	%
metal extracted (bead-to-bead RSD <sup>b</sup> )	29	17	18	34	18	13
metal extracted/bead volume (bead-to-bead RSD <sup>b</sup> )	9	14	10	13	9	16

<sup>a</sup> Poly-L-aspartate ( $n = 20$ ) was immobilized on the beads. <sup>b</sup> Percent RSD values were calculated from the average extract concentrations from seven beads. The metal extract from well no. 5 was not included due to the presence of two beads, giving a larger overall concentration.

the diameters were measured. The beads ranged in size from 85 to 105  $\mu$ m ( $\pm 2 \mu$ m).

The concentration of metal in the extract solution from each bead is shown in Figure 1 along with the bead volumes calculated from the bead diameters. Well no. 5 mistakenly contained two beads ( $d = 90$  and  $98, \pm 2 \mu$ m), and thus, the overall concentration is close to double that of the values in the other seven wells. The figure shows bead extract concentrations as low as 4 ng mL<sup>-1</sup> for Mn<sup>2+</sup> and as high as 130 ng mL<sup>-1</sup> for Cu<sup>2+</sup>, excluding well no. 5; Mg values were omitted from this figure because they were not significantly detectable above the blank levels. Acid introduced into wells containing no bead was used as a control and showed metal signals near the detection limits, indicating that metal contamination from the microwell plate, well cover adhesive, and tweezers was negligible. A small amount of Ni was observed, possibly from the tweezers, but it was only slightly above the limit of detection. The bead-to-bead variation in the average metal content was relatively consistent (also see Table 3), but there was an obvious binding selectivity for certain metals. As might be expected, much of the metal concentration variation in Figure 1 follows that of the bead size.

Due to the variations in bead diameter, the metal extract values from Figure 1 were divided by the volume of the



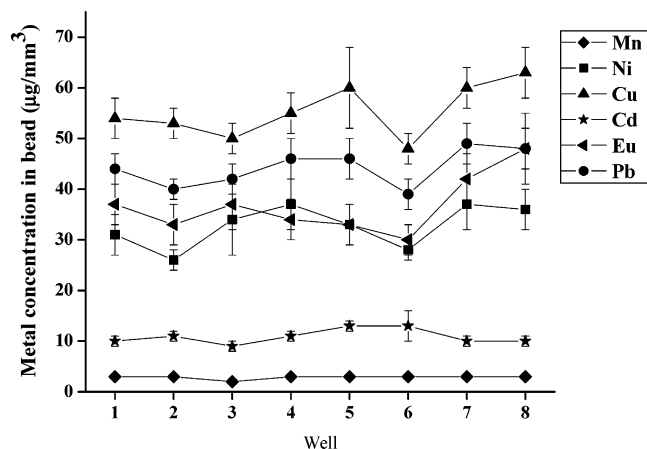


**Figure 2.** Single bead metal extract concentrations of TentaGel–PLAsp normalized to the individual bead volumes. The error bars represent  $\pm 1\sigma$  ( $n = 3$ ) based on error propagated using the analysis error of the sample, blank, and calibration solutions. (Two beads were present in well no. 5.)

respective beads to calculate metal capacities. The standard deviation in the bead diameters was 7% ( $n = 35$ ), which resulted in a 21% RSD in the volumes. When the metal capacities for each bead are normalized by the individual bead volume, a reduction in the bead-to-bead capacity variation (9–16% RSD) is observed. (Figure 2 and Table 3) The more refractory nature of Ni and Eu may account for the somewhat poorer precision between beads for these particular metals even after volume adjustment. The remaining error between capacity values is likely the result of measurement uncertainties in the determination of individual bead capacities.

An attempt was made to identify the possible sources of uncertainty when determining the volume-corrected metal capacity of a single bead. The sources of indeterminate errors (i.e., precision) were analysis error, variation in bead-to-bead binding site density, and error in measuring the bead diameter. The “analysis error” included contributions from the bead extract measurement, blank measurement, and calibration curve slope error and excluded particle diameter measurement and bead-to-bead variations in active site density. An internal standard was used to minimize errors caused by evaporation and sample introduction into the ETV. After volume normalization of the bead set, the relative precision in the capacity (i.e.,  $\mu\text{g}/\text{mm}^3$ ) can be represented by eq 1.

$$\text{RSD}_{\text{capacity}} = \frac{1}{\sqrt{\text{RSD}_{\text{analysis}}^2 + \text{RSD}_{\text{site density}}^2 + 9\text{RSD}_{\text{micrometer}}^2}} \quad (1)$$

It should be noted that propagating the measurement error of the radius (or diameter) to the bead volume yields a volume uncertainty of  $3\text{RSD}_{\text{micrometer}}$ . Error propagation in eq 1 requires summing the squares of the relative error; hence,  $9\text{RSD}_{\text{micrometer}}^2$ . Variations in the site density cannot be measured directly; however, eq 1 can be used to determine if the  $\text{RSD}_{\text{site density}}$  is significant relative to the other RSDs, since they are known. Using 2 m as  $\sigma$  for the micrometer stage error for a 98- $\mu\text{m}$  bead yields 6.1% for  $3\text{RSD}_{\text{micrometer}}$ . Using pooled data for each element,  $\text{RSD}_{\text{analysis}}$  was deter-

mined to be Mn (3%), Ni (11%), Cu (4%), Cd (12%), Pb (4%), and Eu (10%). Finally, the  $\text{RSD}_{\text{capacity}}$  was arrived at from the experimental data for Mn (7%), Ni (13%), Cu (7%), Cd (14%), Pb (7%), and Eu (12%). Using these data, it is obvious that major uncertainties in site density are not required to account for the observed deviations in capacity measurements. Additionally, it can be deduced that analysis precision dominates the uncertainty in the Ni, Cd, and Eu capacities and that analysis and particle diameter imprecision contribute significantly to the uncertainty in the Mn, Cu, and Pb capacities for these beads. The F-test (95% CI) confirmed this conclusion; i.e., only small error contributions arise from errors in determining the bead diameters and negligible contribution comes from binding site density variations. Since no significant error was caused by variation in bead-to-bead differences in site density, all of the beads observed had nearly the same density of active sites. This observation is in agreement with a previous study using confocal Raman microscopy<sup>24</sup> but in disagreement with diffusion studies of Rhodamine 6G through TentaGel.<sup>23</sup>

To determine the amount of metal extracted by the acid soaking procedure, a selection from the PLAsp beads whose acid extract had been previously analyzed were separately analyzed directly in the ETV. In this study, total consumption of the beads was used to ensure that metal was extracted from the beads with acid. Total bead consumption is not necessary if peptide sequencing is desired. After inserting the bead and a small amount of solution into the ETV, the resin material was removed by  $\text{O}_2$  ashing in the ETV at  $\sim 800^\circ\text{C}$ , and the remaining metal was then vaporized and determined via ICPMS. Total metal exposure was calculated by combining the metal amount extracted from the bead with the metal amount remaining on the bead to calculate the total metal on the bead after multimetal exposure. The results for wells 1–4 and 6–7 showed approximately 97, 99, 100, 98, 100, and 100% of Mn, Ni, Cu, Cd, Eu, and Pb, respectively, were released upon acid exposure, which indicates quantitative release of the metals bound to this particular peptide.

**Metal Determination from the Combinatorial Library Beads.** A combinatorial peptide library was then used as an example for determination of selective metal-binding peptides by this method. To minimize analysis error by increasing the signal magnitude, TentaGel Macrobeads were used for the combinatorial library. They were twice the diameter (i.e., 8 times the volume) of those used with the PLAsp but otherwise had the same nominal specification. Measurements of 35 beads showed an average diameter of  $251\ \mu\text{m} \pm 5.4\%$  (i.e.,  $\pm 16\%$  in volume). After exposing the beads to a mixed-metal solution, the library beads were noticeably different in color, ranging from dark red to light blue.

Figure 3 shows the resulting volume-normalized capacities determined for the small set of peptide library beads. Mg values for wells B, C, E, and J were omitted from this figure because they were not significantly detectable above the blank levels. As expected, there are distinct differences in capacities for each element as well as in the relative capacities of one element to another for each bead. For example, beads from wells A and I had the highest capacity for Mg; beads from wells A and F had the highest capacities

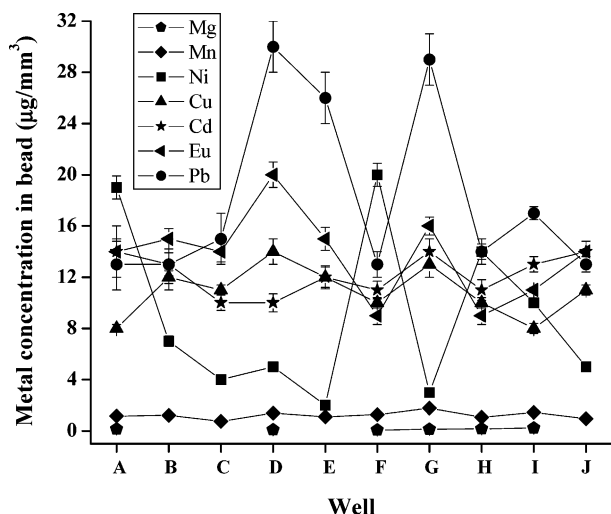


**Figure 3.** Single bead metal extract concentrations of the peptide combinatorial library normalized to the individual bead volumes. The error bars represent  $\pm 1\sigma$  ( $n = 3$ ) based on error propagated using the analysis error of the sample, blank, and calibration solutions. Mg concentration in wells B, C, E, and J was negligible ( $< 0.6 \mu\text{g}/\text{mm}^3$ ).

for Ni; beads from wells D and G had the highest capacities for Cu, Pb, and Eu; and beads from wells G and I had the highest capacities for Mn and Cd. Similarly, if one were in search of a bead that provided good Pb binding capacity with maximum rejection of Ni, bead G from this small set of the library would be the optimal choice.

Since these beads were also measured with the stage micrometer and were manufactured in a similar manner (i.e., similar variation in bead composition), the remaining error after bead volume adjustment can be ascribed primarily to analysis error, since the relative error from the particle diameter uncertainty is smaller for these larger beads. In addition, the precision in these calculated capacities was slightly improved as a result of the higher concentrations extracted from the larger beads as a result of improved measurement precision and less error in measuring the bead diameter: Mg (10%), Mn (3%), Ni (5%), Cu (5%), Cd (6%), Pb (9%) and Eu (7%). In cases in which measuring individual beads diameters would be difficult or excessively time-consuming, larger bead sizes provide a means to decrease the overall concentration uncertainty from bead-to-bead by decreasing the relative analysis error. Obviously, bead sets with better monodispersity could also be used to increase precision if the diameters of individual beads were not measured.

A sample of five library beads was also analyzed directly using ETV after they had been soaked and rinsed in  $\text{HNO}_3$  to see if the acid extraction was complete. Whereas the beads released Mn, Cd, Eu, and Pb with 99–100% efficiency and Mg with 95–100% efficiency,  $\text{Cu}^{2+}$  showed a more varied retention (75, 100, 90, 91, and 97% metal extracted). Since each of these particular beads likely had a unique peptide sequence, it is not unexpected that strong binding sites on any given bead may not release the metal using this particular stripping solution. The beads were not sequenced in this study, since the scope of the work was intended only to demonstrate the viability of using ETV-ICPMS as a metal

screening technique using a small bead set. Although 95+% extraction is probably adequate for screening purposes, perhaps one might be concerned with  $< 80\%$  efficiency, depending on the level of screening being sought. Clearly, total consumption of the bead via oxygen ashing and ETV-ICPMS is not the answer if the peptide sequence is to be determined. It was used in this study only to illustrate that most metal is released by acid extraction. If the peptide is intended to be used as a *reusable* chelating media for metal remediation, one could argue that sites that cannot be reclaimed do not effectively “exist” and, thus, should not be counted in the binding capacity of the material. In these cases, beads with inadequate release should be preferentially *selected against* if the target metal concentration in the extract was low, regardless of how much metal was actually bound to the bead.

### Conclusions

With the exception of metals that are bound tightly to the peptide, acid stripping of the metals in a single bead into a small volume is demonstrated to be a viable quantitative analytical approach when using determination by ETV-ICPMS. Precisions of better than  $\pm 10\%$  were achieved for all metals when the larger polymer beads were employed. Although acid was used in this study, other reclamation (stripping) solutions could be employed, such as a competitive chelator like EDTA. Obviously, the use of different extraction solutions may also yield additional information on the relative strength of binding sites and other characteristics of the peptide sequence. The high sensitivity and low volume requirements of the ETV allow for single beads to be easily analyzed, and the TOF allows for unlimited  $m/z$  monitoring analysis with no sensitivity loss for multi-elemental analysis, since there is no loss in the mass analyzer duty cycle. Though the method presented here could be performed on other types of mass spectrometers (i.e., quadrupoles), the large number of isotopes observed might result in duty-cycle-related losses in sensitivity. For this study, the PLAsp beads and library beads had 21 and 16% variation in the volumes, respectively. This bead-to-bead variability associated with the metal extracted can be corrected for by normalization to the bead volume, with the remaining error primarily ascribed to analysis error, and for the smaller beads, to the particle measurement error. Such volume correction may not be necessary, depending on the monodispersity of the bead set and the acceptable precision limit set by the analyst for the screen. Interestingly, this study does show that bead-to-bead site density variability was not a major contributor to the uncertainty in the overall capacity values for the Tentagel bead sets used.

The 2–3-min analysis time needed for each sample per replicate presently makes this technique suited for quantitative analysis of *selected* beads after an initial bulk screening method. Use of this approach for rapid, quantitative screening may be viable with automation of bead manipulation and an increase in throughput for the ETV-ICPMS. Such has been suggested by work with a multiplexed ETV system,<sup>25,26</sup> in which  $> 100$  analyses/h were reported.

**Acknowledgment.** This work was supported, in part, by the Robert A. Welch Foundation, the Texas Hazardous Waste Research Center and the National Science Foundation (CHE-0315336). We also thank Klaus Linse, Michelle Gadush, and Sandra Smith for their assistance in peptide synthesis and characterization.

### References and Notes

- (1) Breit, B. *Angew. Chem., Int. Ed.* **2005**, *44*, 6816–6825.
- (2) Qi, S.; Yang, B.; Zhuo, Y. *Xiandai Huagong* **2003**, *23*, 58–60.
- (3) Bluhm, L.; Huang, J.; Li, T. *Anal. Bioanal. Chem.* **2005**, *382*, 592–598.
- (4) Kellam, B. *Smith and Williams' Introduction to the Principles of Drug Design and Action*, 4th ed.; CRC/Taylor & Francis: Boca Raton, 2006, pp 355–376.
- (5) Weber, L. *QSAR Comb. Sci.* **2005**, *24*, 809–823.
- (6) Koinuma, H.; Takeuchi, I. *Nat. Mater.* **2004**, *3*, 429–438.
- (7) Woo, S. I.; Kim, K. W.; Cho, H. Y.; Oh, K. S.; Jeon, M. K.; Tarte, N. H.; Kim, T. S.; Mahmood, A. *QSAR Comb. Sci.* **2005**, *24*, 138–154.
- (8) Francis, M. B.; Jamison, T. F.; Jacobsen, E. N. *Curr. Opin. Chem. Biol.* **1998**, *2*, 422–428.
- (9) *Metallothioneins: Synthesis, Structure and Properties of Metallothioneins, Phytochelatins and Metal-Thiolate Complexes*; Stillman, M. J., Shaw, C. F., III, Suzuki, K. T., Eds; John Wiley & Sons: New York, 1992.
- (10) Atherton, E.; Sheppard, R. C. *Solid Phase Peptide Synthesis: A Practical Approach*; IRL Press at Oxford University Press: Oxford, New York, 1989.
- (11) Merrifield, R. B. *J. Am. Chem. Soc.* **1963**, *85*, 2149–2154.
- (12) Francis, M. B.; Finney, N. S.; Jacobsen, E. N. *J. Am. Chem. Soc.* **1996**, *118*, 8983–8984.
- (13) Franz, K. J.; Nitz, M.; Imperiali, B. *ChemBioChem* **2003**, *4*, 265–271.
- (14) Shibata, N.; Baldwin, J. E.; Wood, M. E. *Bioorg. Med. Chem. Lett.* **1997**, *7*, 413–416.
- (15) Pirrung, M. C.; Park, K.; Tumej, L. N. *J. Comb. Chem.* **2002**, *4*, 329–344.
- (16) Neilly, J. P.; Hochlowski, J. E. *Appl. Spectrosc.* **1999**, *53*, 74–81.
- (17) Miller, T. C.; Mann, G.; Havrilla, G. J.; Wells, C. A.; Warner, B. P.; Baker, R. T. *J. Comb. Chem.* **2003**, *5*, 245–252.
- (18) Minogue, E. M.; Havrilla, G. J.; Taylor, T. P.; Burrell, A. K.; Warner, B. P. *Proc. SPIE Int. Soc. Opt. Eng.* **2005**, 5699, 526–530.
- (19) Vazquez Pelaez, M.; Costa-Fernandez, J. M.; Sanz-Medel, A. *J. Anal. At. Spectrom.* **2002**, *17*, 950–957.
- (20) Stair, J. L.; Holcombe, J. A. *Microchem. J.* **2005**, *81*, 69–80.
- (21) Malachowski, L.; Stair, J. L.; Holcombe, J. A. *Pure Appl. Chem.* **2004**, *76*, 777–787.
- (22) Langer, D.; Holcombe, J. A. *Anal. Chem.* **1999**, *71*, 582–588.
- (23) Taniguchi, M. M.; Farrer, R. A.; Fourkas, J. T. *J. Comb. Chem.* **2005**, *7*, 54–57.
- (24) Kress, J.; Zanaletti, R.; Rose, A.; Frey, J. G.; Brocklesby, W. S.; Ladlow, M.; Bradley, M. *J. Comb. Chem.* **2003**, *5*, 28–32.
- (25) Venable, J. D.; Detwiler, M.; Holcombe, J. A. *Spectrochim. Acta, Part B* **2001**, *56B*, 1697–1706.
- (26) Kreschollek, T.; Holcombe, J. A., *32nd Meeting of the Federation of Analytical Chemistry & Spectroscopy Societies (FACSS)*, Quebec City, Canada, October 9–13, 2005; p 204.

CC060100M